Available online at www.sciencedirect.com
ScienceDirect
Journal of Molecular Catalysis A: Chemical 275 (2007) 167–173
JOURNAL OF MOLECULAR CATALYSIS A: CHEMICAL
www.elsevier.com/locate/molcata

Silica supported ceria and ceria–zirconia nanocomposite oxides for selective dehydration of 4-methylpentan-2-ol

Benjaram M. Reddy *, Gode Thrimurthulu, Pranjal Saikia, Pankaj Bharali

Inorganic and Physical Chemistry Division, Indian Institute of Chemical Technology, Uppal Road, Hyderabad 500007, India

Received 25 April 2007; received in revised form 21 May 2007; accepted 21 May 2007
Available online 31 May 2007

Abstract

Selective dehydration of 4-methylpentan-2-ol to 4-methylpent-1-ene has been investigated over SiO_2 supported CeO_2 and $Ce_xZr_{1-x}O_2$ nanocomposite oxides in the vapour phase under normal atmospheric pressure. The investigated supported nano-oxides were synthesized by a co-precipitation method from ultrahigh dilute aqueous solutions of nitrate precursors and colloidal silica. Physicochemical characterization was achieved by X-ray powder diffraction, Raman spectroscopy, high-resolution transmission electron microscopy and BET surface area techniques. XRD measurements revealed the formation of nanosized cubic crystallites of CeO_2 and $Ce_{0.75}Zr_{0.25}O_2$ in CeO_2/SiO_2 and $Ce_xZr_{1-x}O_2/SiO_2$ catalysts, respectively. The Raman studies provided evidence for the formation of oxygen vacancies in both the catalysts. The HRTEM results revealed that SiO_2 acts as an inert support to stabilize the formed nanosized cubic crystallites of CeO_2 and Ce–Zr-oxides (~3–5 nm) in case of CeO_2/SiO_2 and $Ce_xZr_{1-x}O_2/SiO_2$ samples, respectively. The conversion of 4-methylpentan-2-ol was increased to some extent when CeO_2 was dispersed over SiO_2. After incorporation of Zr^{4+} to CeO_2/SiO_2, the conversion was found to increase to a greater extent. The selectivity of the desired product 4-methylpent-1-ene was observed to be highly dependent on the reaction temperature.

Keywords: CeO_2/SiO_2; $Ce_xZr_{1-x}O_2/SiO_2$; Dehydration; 4-Methylpentan-2-ol; Catalyst characterization

1. Introduction

Ceria (CeO_2) is an interesting oxide industrially, applied widely in catalysis, material science, fuel cell processes and gas sensor technologies [1,2]. In recent years, ceria and ceria-based composite oxides have been extensively investigated for variety of reactions such as preferential oxidation of CO [3,4], steam reforming of ethanol [5], synthesis of dimethylcarbonate from methanol and CO_2 [6], direct conversion of methane to synthesis gas [7], iso-synthesis [8], dehydration of alcohols [9–12], oxidative dehydrogenation of ethylbenzene [13] and low-temperature water-gas shift reaction [1], apart from the conventional three-way catalytic applications to reduce the emissions of noxious pollutants such as CO, NO_x and hydrocarbons from automobile exhausts [14,15]. The redox and oxygen storage/release properties of ceria play a major role in most of these applications. There are few attempts in the literature on the application of CeO_2–ZrO_2 and CeO_2–La_2O_3 composite oxides for dehydration of 4-methylpentan-2-ol to 4-methylpent-1-ene and also to evaluate the surface acid–base properties of these and other catalysts [9,10,12]. In fact, acid–base and redox properties of metal oxides play a vital role in catalysis and there are several chemical processes that have been industrially exploited for various applications based on surface acid–base sites of the metal oxide catalysts [16–21]. The dehydration of 4-methylpentan-2-ol could represent an alternative route to the preparation of 4-methylpent-1-ene, a starting material for the manufacture of thermoplastic polymers of high technological significance. Besides the desired 4-methylpent-1-ene, the alcohol dehydration always leads to formation of 4-methylpent-2-ene, often accompanied by skeletal isomers of C_6-alkenes and dehydrogenated product 4-methylpentan-2-one [10]. It was noticed in earlier studies that the CeO_2–ZrO_2 catalysts exhibit good catalytic activity with high product selectivity towards the desired 4-methylpent-1-ene [9]. They also help to avoid the formation of olefins with internal double bonds and the dehydrogenation product, ketone [9]. It is a known fact that unsupported

* Corresponding author. Tel.: +91 40 2716 0123; fax: +91 40 2716 0921.
E-mail addresses: bmreddy@iict.res.in, mreddyb@yahoo.com (B.M. Reddy).

1381-1169/$ – see front matter © 2007 Elsevier B.V. All rights reserved.
doi:10.1016/j.molcata.2007.05.037

forms of ceria and its composite oxides possess several disadvantages such as low specific surface area, low thermal and structural/textural stability leading to easy sintering under high temperature applications. Therefore, there are some attempts in the recent literature to disperse ceria-based nanocomposites on different supports and exploit them for various catalytic reactions [13,22–25]. Silica is one of the most widely used inert supports with high specific surface area and high thermal stability which is known to enhance the dispersion and catalytic activity of most of the deposited active oxides. However, there are no such attempts in the literature to exploit it for ceria-based nanocomposite oxides for different catalytic applications.

The present investigation was undertaken against the above background. In this study highly dispersed nano-oxides of CeO_2 and $Ce_xZr_{1-x}O_2$ over silica support have been synthesized and investigated for selective dehydration of 4-methylpentan-2-ol to 4-methylpent-1-ene in the vapour phase under normal atmospheric pressure. The CeO_2/SiO_2 and $Ce_xZr_{1-x}O_2/SiO_2$ nanocomposite oxides were prepared by a deposition co-precipitation method and the physicochemical characterization was carried out by X-ray diffraction, Raman spectroscopy, high-resolution transmission electron microscopy and BET surface area techniques. An unsupported CeO_2 was also prepared and investigated for the purpose of comparison.

2. Experimental

2.1. Catalyst preparation

The CeO_2/SiO_2 (C/S; 1:1 mole ratio based on oxides) and $Ce_xZr_{1-x}O_2/SiO_2$ (CZ/S; 1:1:2 mole ratio based on oxides) catalysts were prepared by a deposition co-precipitation method. A pure CeO_2 (C) was also prepared by precipitation technique. The precursors used were $(NH_4)_2Ce(NO_3)_6$ (Loba Chemie, GR grade), $Zr(NO_3)_4{\cdot}5H_2O$ (Fluka, AR grade) and colloidal SiO_2 (Ludox, 40 wt.%, Aldrich, AR grade). Aqueous NH_3 solution was used as precipitating agent. To prepare C/S and CZ/S samples, colloidal SiO_2 was first dispersed in 3000 ml deionized water and stirred for 2 h. To this dispersed content, mixture solutions of cerium and zirconium precursors were added and stirred for 1 h. Aqueous NH_3 solution was added dropwise to the aforementioned mixture solutions until pH ~ 8.5 under vigorous stirring conditions. The obtained precipitates were filtered off, washed with deionized water until free from anion impurities and oven dried at 393 K for 12 h and subsequently calcined at 773 K for 5 h.

2.2. Catalyst characterization

X-ray powder diffraction patterns were recorded on a Siemens D-500 diffractometer using nickel-filtered Cu Kα (0.15418 nm) radiation source. Crystalline phases were identified by comparison with the reference data from PDF-ICDD files. The average crystallite size was estimated with the help of Scherrer equation. The Raman spectra were recorded on a DILOR XY spectrometer equipped with a liquid N_2 cooled CCD detector at ambient temperature and pressure. The emission line at 514.5 nm from an Ar^+ ion laser (Spectra Physics) was focused on the sample (analyzing spot 1 μm) under microscope. The power of incident beam on the sample was 3 mW and time of acquisition varied according to the intensity of the Raman scattering. The wavenumbers obtained from spectra are accurate to within 2 cm^{-1}. The HRTEM images were recorded with a JEM 2010 (Cs = 0.5 mm) microscope. The accelerating voltage was 200 kV with LaB_6 emission current with a point resolution of 0.195 nm. Samples were sonically dispersed in ethanol and deposited on a holey carbon copper grid before examination. The BET surface areas were obtained by N_2 physisorption on a Micromeritics Gemini 2360 Instrument. Before measurements, the samples were oven dried at 393 K for 12 h and flushed with Argon gas for 2 h.

2.3. Activity studies

Catalytic activity measurements were carried out at 523–673 K, in a down flow fixed-bed micro-reactor heated by means of a tubular furnace in a previously described apparatus [12,13]. The reactor–catalyst load consisted of 0.5 g of catalyst diluted with quartz fractions. The catalyst was treated using CO_2-free airflow at 773 K for 5 h, prior to the reaction. The 4-methylpentan-2-ol was fed with N_2 stream, into the vaporizer at a flow rate of 1.5 ml h^{-1}. The flow rate of dry N_2 was maintained at 60–70 ml min^{-1}. The liquid products were collected in ice-cold freezing traps and were analyzed by a gas chromatograph with flame ionization detector (FID). The qualitative analysis of the products was performed with the help of NMR and Mass spectrometry techniques. The activity data was collected under steady state conditions. The conversions and product selectivity were calculated as per the procedure described elsewhere [26].

3. Results and discussion

The XRD profiles of C, C/S and CZ/S samples calcined at 773 K are presented in Fig. 1. The diffraction profiles of C/S and CZ/S are relatively broad in comparison to C indicating

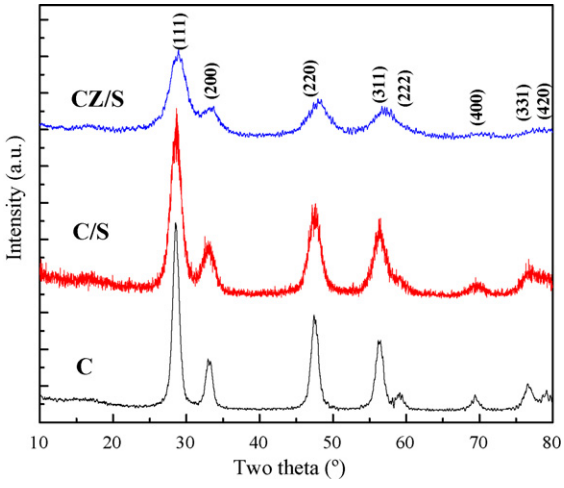

Fig. 1. X-ray powder diffraction profiles of CeO_2 (C), CeO_2/SiO_2 (C/S) and $Ce_xZr_{1-x}O_2/SiO_2$ (CZ/S) samples.

smaller particle sizes. All the diffraction peaks could be indexed to (1 1 1), (2 0 0), (2 2 0), (3 1 1), (2 2 2), (4 0 0), (3 3 1) and (4 2 0) crystal faces, corresponding to a face centered cubic fluorite structure of CeO_2. From Fig. 1, it could be observed that pure ceria and C/S crystallize only as cubic CeO_2 (PDF-ICDD 34-0394). In the case of CZ/S, presence of cubic Ce–Zr-oxide with the composition namely, $Ce_{0.75}Zr_{0.25}O_2$ (PDF-ICDD 28-0271) has been identified. No other crystalline phases were observed which correspond to catalytically inert compounds or mixed oxide phases between ceria–silica and silica–zirconia in the present study in contrast to some other earlier reports [27,28]. This can be attributed to a different preparation method adopted and a lower calcination temperature employed in the present study.

The N_2 BET surface areas of all the samples and average crystallite size, as determined from XRD data, of CeO_2 in pure C and C/S, and $Ce_{0.75}Zr_{0.25}O_2$ in CZ/S are presented in Fig. 2. A substantial increase in the surface area and decrease in the particle size could be observed when the amorphous silica support was introduced. This indicates that the high surface area silica support enhances the effective dispersion and stabilization of C and CZ particles over its surface. The use of colloidal silica as inert support further helps to crystallize C and CZ oxides with particle sizes in the nanometer range. There are certain advantages associated with the use of colloidal silica dispersions. Firstly, the colloidal dispersions are much less reactive toward the deposited catalytic materials, and as a consequence, solid-state reactions are less likely to occur with the colloidal materials than with the coprecipitated materials from the soluble salts. Secondly, the particles of the colloids are larger than the particles of the coprecipitated salts. This has a feature of making larger pores and more open structures for the final catalyst. Thus, the precipitation of ceria and ceria–zirconia with colloidal silica yielded smaller crystallites of C and CZ oxides on the surface of SiO_2. Therefore, the colloidal silica support has been advantageously employed in the present investigation. The term colloidal silica refers to a stable, dispersion or sols of discrete nanometric particles of amorphous silica, commonly suspended in water with a size of about 7–12 nm in diameter. Depending

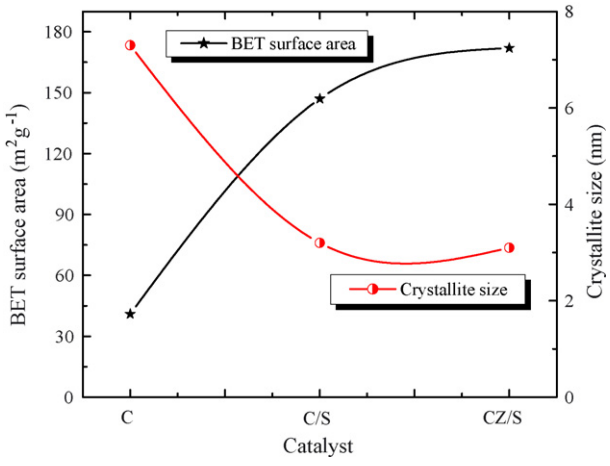

Fig. 2. BET surface area and average crystallite size of CeO_2 (C), CeO_2/SiO_2 (C/S) and $Ce_xZr_{1-x}O_2/SiO_2$ (CZ/S) samples.

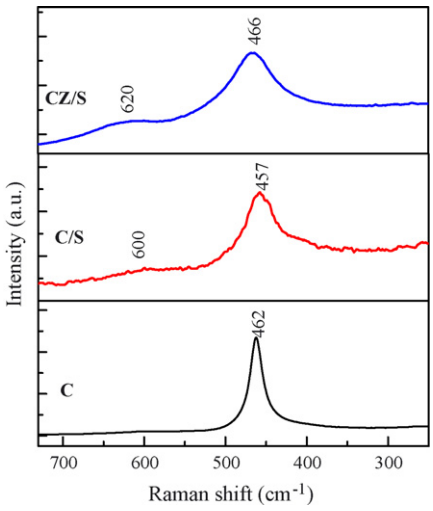

Fig. 3. Raman spectra of CeO_2 (C), CeO_2/SiO_2 (C/S) and $Ce_xZr_{1-x}O_2/SiO_2$ (CZ/S) samples.

on the synthesis conditions, the structure of the colloidal particles may differ from isolated spherical particles to agglomerates of complex structures. Colloidal silica also exhibits reasonably high specific surface area ranging between 140 and 345 $m^2\,g^{-1}$.

The Raman spectra of C, C/S and CZ/S samples are presented in Fig. 3. The Raman spectrum of pure CeO_2 displays only one prominent peak at 462 cm^{-1} due to F_{2g} Raman active mode of the fluorite structure [22,25,29,30]. The absence of any other features in the spectra indicates the non-existence of structural defects or oxygen vacancies in the pure CeO_2. The Raman spectrum of C/S shows a prominent peak at 457 cm^{-1} and a weak band at ~600 cm^{-1}. The band at 457 cm^{-1} corresponds to the triply degenerate F_{2g} mode and can be viewed as a symmetric breathing mode of the oxygen atoms around cerium ions [31]. In the case of CZ/S sample, the band due to F_{2g} mode has been observed at 466 cm^{-1}. It is well reported in the literature that intensity of Raman band depends on several factors including grain size and morphology. The weak bands noticed for C/S and CZ/S at ~600 and 620 cm^{-1}, respectively, correspond to a non-degenerate LO mode of CeO_2 [32,33]. Normally, this mode should not be observed by Raman spectroscopy but the presence of some defects can involve relaxation of selection rules. In particular, this band has been linked to oxygen vacancies in the CeO_2 lattice [34]. The absence of any other Raman features provides one more inference that silica is not forming any compound with ceria or zirconia, in line with XRD measurements.

The TEM-HREM studies were performed on some selected representative samples to ascertain the structural information obtained from XRD and Raman measurements. The TEM global view of the C/S sample is shown in Fig. 4a. A closer inspection of the image reveals the existence of smaller crystals (~3–5 nm) dispersed over an amorphous matrix with different contrasts. The corresponding HRTEM image (Fig. 4b) of the sample shows that the contrast observed in the experimental image is associated with the face centered cubic fluorite structure of CeO_2. Well-crystallized CeO_2 grains mixed with amorphous SiO_2 are mainly observed [25,27,35,36]. The digital diffraction pattern (DDP)

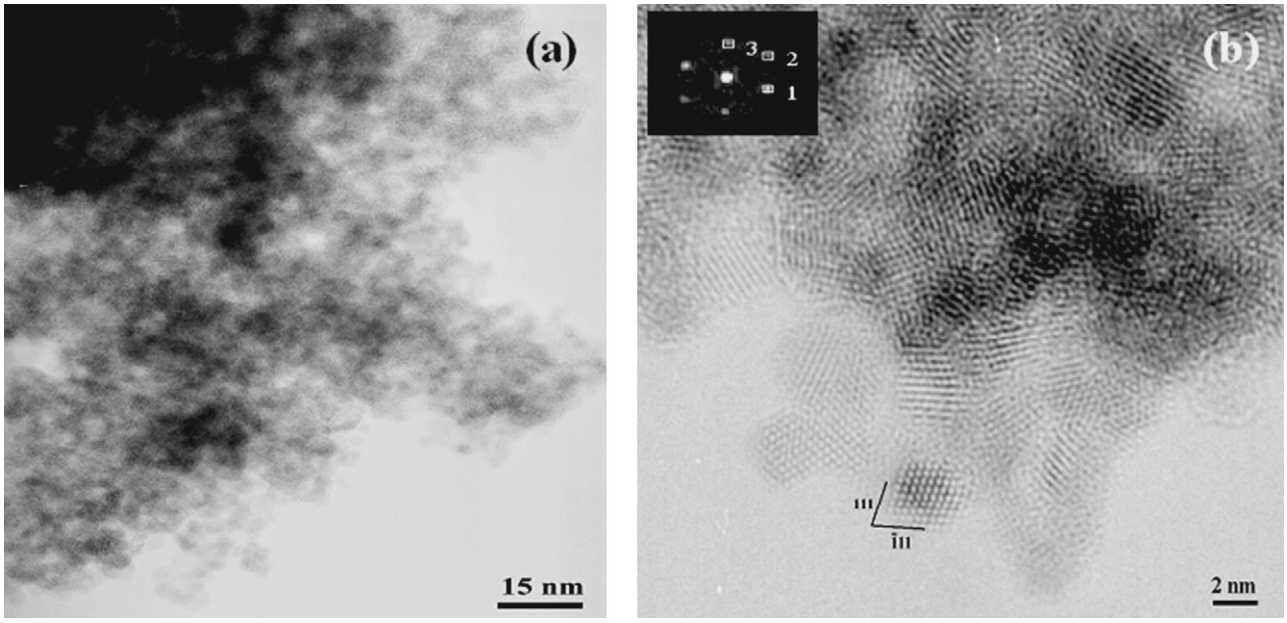

Fig. 4. (a) TEM and (b) HRTEM images of CeO_2/SiO_2 (C/S) sample (inset: digital diffraction pattern obtained from the experimental image).

obtained from the experimental image is also shown in Fig. 4b (inset). The different spots observed account for the existence of periodic contrasts in the original experimental micrograph, which correspond to different sets of atomic planes of the crystalline structure. The geometric arrangement of these reflections is directly related to the structural aspects of the analyzed crystals. The spots labeled as 1, 2, and 3 in the DDP correspond to the interplanar spacings of 3.2, 2.7 and 3.1 Å, respectively, which correspond to the (1 1 1), (2 0 0) and (1 −1 −1) planes of ceria in cubic fluorite structure. TEM global picture of the CZ/S sample along with the corresponding selected area diffraction pattern (SAED) are shown in Fig. 5a. A closer view of the image reveals the existence of small crystals (∼5 nm) dispersed over an amorphous matrix with different lighter contrasts. The broadening of the rings in the electron diffraction patterns account for the presence of such small randomly oriented mixed oxide particles. Well-dispersed very small Ce–Zr-oxide particles over the surface of the amorphous silica are mainly observed from HRTEM image (Fig. 5b). The HRTEM studies thus provide valuable information on the structure of C and CZ oxides, highly dispersed over amorphous silica support in line with XRD and Raman measurements.

The conversion of 4-methylpentan-2-ol produces mainly 4-methylpent-1-ene and 4-methylpent-2-ene with trace amounts

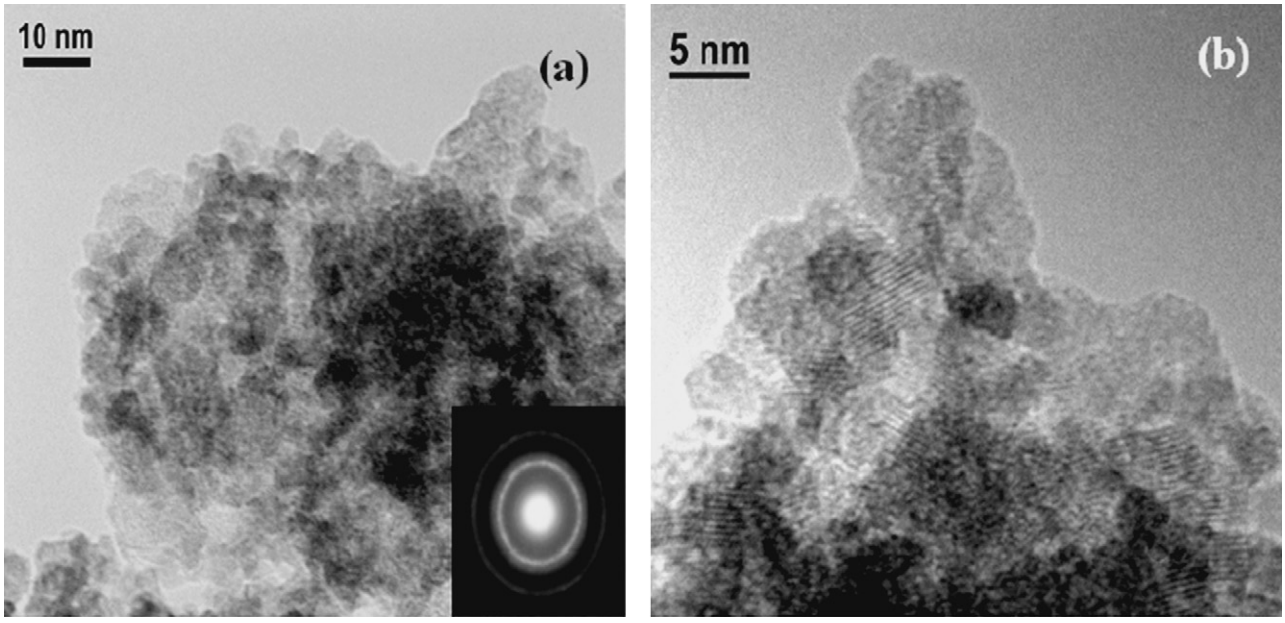

Fig. 5. (a) TEM (inset: selected area diffraction pattern) and (b) HRTEM images of $Ce_xZr_{1-x}O_2/SiO_2$ (CZ/S) sample.

of C_6 alkenes as dehydration products. Besides dehydration, dehydrogenation of the reactant alcohol gives rise to 4-methylpentan-2-one and higher ketones (in very low amounts). Previous works on zirconia, ceria and lanthana-based oxides revealed the involvement of three different mechanistic pathways (E1cB, E1 and E2) to form the desired and undesired products [9–12]. When the acid and base functions of the catalyst are well balanced in terms of site concentrations, a two-point adsorption of the reactant alcohol occurs, in which the most acidic hydrogen (i.e., H of terminal methyl group) interacts with a base site while the acid centre interacts with the OH group of the alcohol. The fate of this adsorbed species depends on the relative strength of the acid and base sites. If the acid sites are weak and the base sites are strong enough, rupture of the C–H bond with carbanion formation occurs first and an E1cB mechanism sets in leading to the preferential formation of 1-alkene (Hofmann product). If the strengths of the acid and base sites are comparable, no intermediate carbanion is formed. In this situation, the transformation of the adsorbed species into the olefin takes place via concerted mechanism (E2 pathway) and 2-alkene is then the preferred product (Saytzeff product). Such co-operative action of the sites is disfavored when either the acid or the base sites are predominant. In the former case, the reaction is initiated by the attack of the acid sites to the hydroxy group of the alcohol leading to the formation of a carbocation intermediate, which transforms into alkenes with internal double bonds (E1 mechanism, Saytzeff product). When the base sites on the catalyst surface are predominant and strong, adsorption occurs by means of a hydrogen bond involving the OH group of the alcohol and a base site. Here abstraction of α-H by interaction with a positively polarized H atom on the surface (originating from the previously split OH group of the alcohol) occurs and a ketone is formed instead of an alkene.

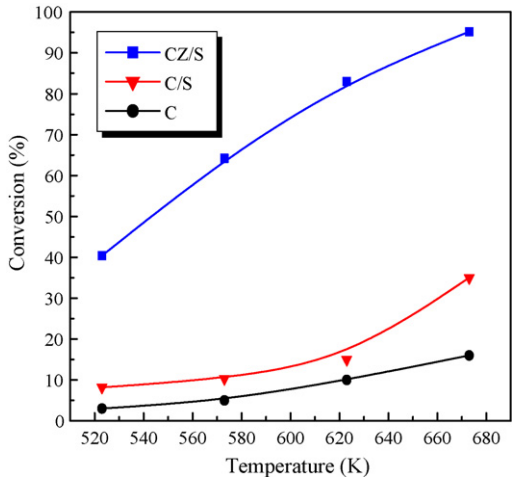

Fig. 6. Conversion of 4-methylpentan-2-ol as a function of reaction temperature over CeO_2 (C), CeO_2/SiO_2 (C/S) and $Ce_xZr_{1-x}O_2/SiO_2$ (CZ/S) catalysts.

Based on the above ideas we have investigated the dehydration of 4-methylpentan-2-ol over C, C/S and CZ/S samples. The conversion of 4-methylpentan-2-ol over the catalysts as a function of reaction temperature is presented in Fig. 6. As shown in the figure, the conversion of alcohol increases with increasing reaction temperature for all the three catalysts. Up on dispersing ceria over SiO_2, the conversion of the alcohol is increased to a little extent, but after incorporation of Zr^{4+} to CeO_2/SiO_2,

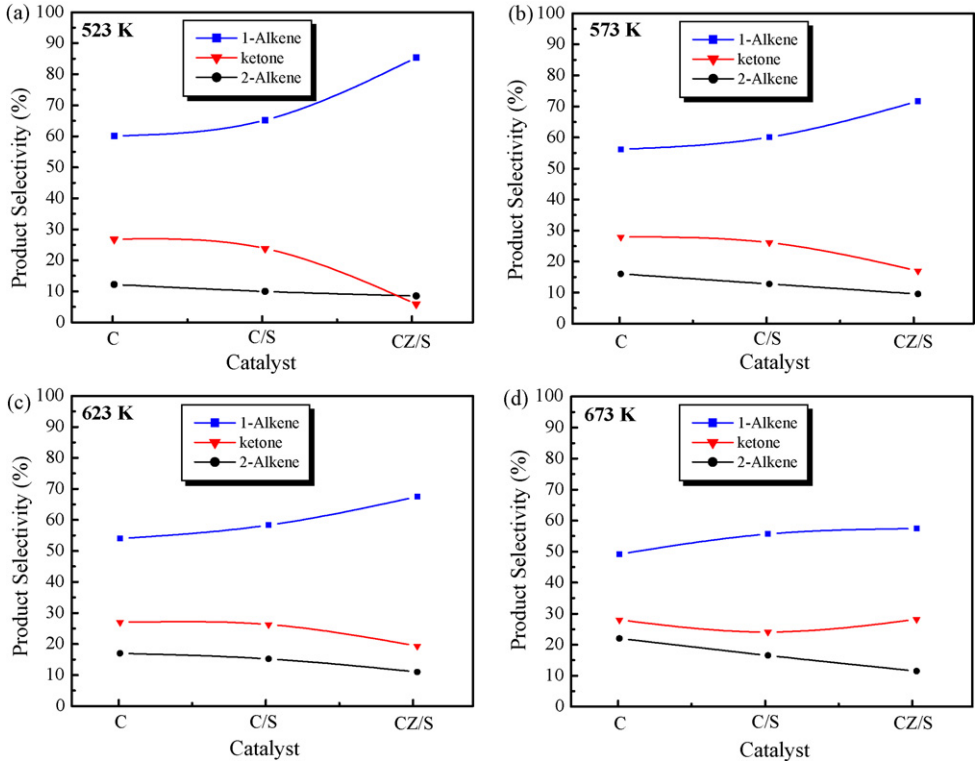

Fig. 7. Selectivities to 4-methylpent-1-ene (1-alkene), 4-methylpent-2-ene (2-alkene) and 4-methylpentan-2-one (ketone) at different temperatures over CeO_2 (C), CeO_2/SiO_2 (C/S) and $Ce_xZr_{1-x}O_2/SiO_2$ (CZ/S) catalysts.

the conversion is drastically increased. A nominal conversion of 8% was observed over C/S at 523 K, the lowest reaction temperature studied, which increased to 35% at 673 K. After Zr^{4+} incorporation to C/S, the conversion raised from 40% at 523 K to 95% at 673 K. The selectivities of the reaction products, 4-methylpent-1-ene (1-alkene; desired product), 4-methylpent-2-ene (2-alkene) and 4-methylpentan-2-one (ketone) over all the catalysts at different temperatures are presented in Fig. 7. As can be seen from this figure, the selectivity of the desired product, 1-alkene increases from pure ceria to CZ/S and decreases with increasing reaction temperature for all the catalysts. On the other hand, the selectivity of the dehydrogenation product, 4-methylpentan-2-one increases with increasing reaction temperature for all the samples, which leads to a decrease in the selectivity of the desired product. However, there is no appreciable change in the selectivity of 4-methylpent-2-ene with increasing reaction temperature for all the catalysts. The present study indicates the involvement of the E1cB mechanistic pathway through the formation of carbanion intermediate to form the highly selective 1-alkene.

The following observations could be related to the highly dispersed ceria and Ce–Zr-oxides over SiO_2 with balanced acid–base and redox sites. The high dispersion of CeO_2 over SiO_2 to form ceria crystallites of ~3–5 nm size accounts for an increase in the conversion of the alcohol, as high dispersion of active oxide always provides more active sites for the reactant molecules to interact. By incorporating Zr^{4+} to C/S, a more balanced acid–base surface sites could be generated which result in a large increase of conversion. Simultaneously, after Zr^{4+}-ion incorporation, the redox behaviour of C/S is also changed with the formation of oxygen vacancies as demonstrated by Raman measurements. The emergence of Raman band at $\sim 600\,cm^{-1}$ is related to the oxygen vacancy concentration, which is more prominent in the case of CZ/S sample. The formation of oxygen vacancy in CZ/S provides more Ce^{3+} sites, which may lead to an increase in the ability of O^{2-} ions to abstract a proton in comparison to the O^{2-} ions connected to Ce^{4+}. This facilitates the E1cB mechanistic pathway to form the desired 1-alkene selectively. Further investigations are necessary to understand the nature of acid–base sites of these catalysts and their role on the conversion and selectivity of this important reaction.

4. Conclusions

Silica supported nanosized CeO_2 and $Ce_xZr_{1-x}O_2$ composite oxides have been synthesized and characterized by XRD, Raman, HRTEM and BET surface area methods. XRD results revealed the formation of cubic CeO_2 in the case of CeO_2/SiO_2 and $Ce_{0.75}Zr_{0.25}O_2$ phase in case of $Ce_xZr_{1-x}O_2/SiO_2$ catalysts. Raman measurements showed the presence of oxygen vacancies and lattice defects in the case of silica supported composite oxides. HRTEM studies disclosed the presence of ceria and Ce–Zr-oxide nanocrystallites of the size ~3–5 nm over the amorphous silica matrix. The conversion of 4-methylpentan-2-ol to 4-methylpent-1-ene is enhanced after Zr^{4+}-ion incorporation to the CeO_2/SiO_2 composite oxide. The selectivity to 1-alkene has been observed to decrease with increasing reaction temperature, while 4-methylpentan-2-one selectivity increases. Further studies are essential to fully exploit these catalysts for the title reaction.

Acknowledgements

Thanks are due to Dr. S. Loridant, IRCELYON, France and Dr. C.L. Cartes, CSIC-UNSE-Sevilla, Spain, for providing Raman and electron microscopy results, respectively. GT, PS and PB thank Council of Scientific and Industrial Research (CSIR), New Delhi, for junior research fellowships. Financial support received from Department of Science and Technology, New Delhi, under SERC Scheme (SR/S1/PC-31/2004).

References

[1] A. Trovarelli, in: G.J. Hutchings (Ed.), Catalysis by Ceria and Related Materials, Catalytic Science Series, vol. 2, Imperial College Press, London, 2002.
[2] R.D. Monte, J. Kaspar, J. Mater. Chem. 15 (2005) 633.
[3] A. Martinez-Ariaz, M. Fernandez-Garcia, A. Iglesias Juez, A.B. Hungria, J.A. Anderson, J.C. Conesa, J. Soria, Appl. Catal. B: Environ. 31 (2001) 51.
[4] B.M. Reddy, P. Bharali, P. Saikia, A. Khan, S. Loridant, M. Muhler, W. Grünert, J. Phys. Chem. C 111 (2007) 1878.
[5] D. Srinivas, C.V.V. Satyanarayana, H.S. Potdar, P. Ratnasamy, Appl. Catal. A: Gen. 246 (2003) 323.
[6] K. Tomishige, K. Kunimori, Appl. Catal. A: Gen. 237 (2002) 103.
[7] K. Otsuka, Y. Wang, M. Nakamura, Appl. Catal. A: Gen. 183 (1999) 317.
[8] Y. Li, D. He, Q. Zhu, X. Zhang, B. Xu, J. Catal. 221 (2004) 584.
[9] M.G. Cutrufello, I. Ferino, V. Solinas, A. Primavera, A. Trovarelli, A. Auroux, C. Picciau, Phys. Chem. Chem. Phys. 1 (1999) 3369.
[10] M.G. Cutrufello, I. Ferino, R. Monaci, E. Rombi, V. Solinas, Top. Catal. 19 (2002) 225.
[11] V. Solinas, E. Rombi, I. Ferino, M.G. Cutrufello, G. Colon, J.A. Navio, J. Mol. Catal. A: Chem. 204-205 (2003) 629.
[12] B.M. Reddy, P. Lakshmanan, P. Bharali, P. Saikia, J. Mol. Catal. A: Chem. 258 (2006) 355.
[13] B.M. Reddy, P. Lakshmanan, S. Loridant, Y. Yamada, T. Kobayashi, C.L. -Cartes, T.C. Rojas, A. Fernandez, J. Phys. Chem. B 110 (2006) 9140.
[14] A. Trovarelli, C. de Leitenburg, G. Dolcetti, Chemtech 27 (1997) 321.
[15] M. Ozawa, K. Matuda, S. Suzuki, J. Alloys Compd. 303–304 (2000) 56.
[16] J.L.G. Fierro (Ed.), Metal Oxides: Chemistry and Applications, CRC Press, Florida, 2006.
[17] M.C. Kung, H.H. Kung, Catal. Rev. Sci. Eng. 27 (1985) 425.
[18] B.M. Reddy, in: J.L.G. Fierro (Ed.), Metal Oxides: Chemistry and Applications, CRC Press, Florida, 2006, p. 215 (Chapter 8).
[19] K. Tanabe, Solid Acid and Bases, Kodansha, Tokyo and Academic Press, New York, 1970.
[20] K. Tanabe, M. Misono, Y. Ono, H. Hattori, New Solid Acid and Bases, Kodansha, Tokyo and Elsevier, Amsterdam, 1989.
[21] J.M. Winterbottom, Catalysis, Specialist Periodical Reports, vol. 4, The Royal Society of Chemistry, London, 1981.
[22] B.M. Reddy, A. Khan, Y. Yamada, T. Kobayashi, S. Loridant, J.-C. Volta, J. Phys. Chem. B 106 (2002) 10964.
[23] B.M. Reddy, A. Khan, Y. Yamada, T. Kobayashi, S. Loridant, J.-C. Volta, J. Phys. Chem. B 107 (2003) 5162.
[24] B.M. Reddy, A. Khan, Y. Yamada, T. Kobayashi, S. Loridant, J.-C. Volta, Langmuir 19 (2003) 3025.
[25] B.M. Reddy, A. Khan, P. Lakshmanan, M. Aouine, S. Loridant, J.-C. Volta, J. Phys. Chem. B 109 (2005) 3355.
[26] B.M. Reddy, M.V. Kumar, K.J. Ratnam, Appl. Catal. A: Gen. 181 (1999) 77.
[27] E. Rocchini, A. Trovarelli, J. Llorca, G.W. Graham, W.H. Weber, M. Maciejewski, A. Baiker, J. Catal. 194 (2000) 461.

[28] E. Rocchini, M. Vicario, J. Llorca, C. de Leitenburg, G. Dolcetti, A. Trovarelli, J. Catal. 211 (2002) 407.
[29] A. Martinez-Arias, M. Fernandez-Garcia, L.N. Salamanca, R.X. Valenzuela, J.C. Conesa, J. Soria, J. Phys. Chem. B 104 (2000) 4038.
[30] J.Z. Shyu, W.H. Weber, H.S. Gandhi, J. Phys. Chem. 92 (1988) 4964.
[31] X.-M. Lin, L.-P. Li, G.-S. Li, W.-H. Su, Mater. Chem. Phys. 69 (2001) 236.
[32] T. Hirata, E. Asari, M. Kitajima, J. Solid State Chem. 110 (1994) 201.
[33] V.S. Escribano, E.F. Lopez, M. Panizza, C. Resini, J.M.G. Amores, G. Busca, Solid State Sci. 5 (2003) 1369.
[34] J.R. McBride, K.C. Hass, B.D. Poindexter, W.H. Weber, J. Appl. Phys. 76 (1994) 2435.
[35] L. Lepinski, M. Wolcyrz, J. Solid State Chem. 131 (1997) 121.
[36] L. Lepinski, M. Wolcyrz, M. Marchewka, J. Solid State Chem. 168 (2002) 110.